

Wobbling double sine-Gordon kinks

João G. F. Campos

Departamento de Física, Universidade Federal de Pernambuco,
Av. Prof. Moraes Rego, 1235, Recife - PE - 50670-901, Brazil
joao.gfcampos@ufpe.br

Azadeh Mohammadi

Departamento de Física, Universidade Federal de Pernambuco,
Av. Prof. Moraes Rego, 1235, Recife - PE - 50670-901, Brazil
azadeh.mohammadi@ufpe.br

February 28, 2025

Abstract

We study the collision of a kink and an antikink with the excited vibrational mode in the double sine-Gordon model. The vibrational energy of the wobbling kinks can turn into translational energy after the collision. This creates one-bounce as well as a rich structure of higher-bounce resonance windows that depend on the wobbling phase is in or out of phase at the collision, and the wobbling amplitude is sufficiently large. This structure of one- and higher-bounce windows are observed for a wide range of the model's parameters. We estimated the center of the one-bounce windows using a simple analytical approximation for the wobbling evolution. The kinks' final wobbling frequency is Lorentz contracted, which is simply derived from our equations. We also report that the maximum value of the energy density always has a smooth behavior in the resonance windows.

1 Introduction

Solitons, instantons and monopoles for instance, are important solutions of field theories that appear when the configuration of the system at the boundary is topologically nontrivial [1,2]. In particular, soliton solutions of relativistic scalar field theories in $(1+1)$ dimensions are called kink and antikink. The degeneracy of the potential is essential for their existence. These solutions appear in the description of many physical systems such as polyacetylene [3], Josephson junctions [4], graphene deformations [5], domain walls in ferromagnets [6] and Helium-3 [7].

Two of the most studied models in the field are the sine-Gordon and the ϕ^4 . The sine-Gordon is integrable, giving rise to what is called a true soliton. The ϕ^4 , on the other hand, is non-integrable and exhibits a much wider variety of outcomes. In the former, the collision between the kinks is always elastic, and the only effect of the interaction is a phase shift in the kinks propagation. In the latter, the constituents in a kink-antikink collision may instead reflect inelastically or annihilate. Moreover, it may also happen that the solitons separate after more than one-bounce in what is called resonance windows. This interesting phenomenon has been extensively studied for a few decades and is still not completely understood.

Historically, the pioneering works about kink-antikink collisions include Sugiyama [8], Campbell et al. [9–11]. and Anninos et al. [12]. In [8], the author observed that, after

the collision, a kink and an antikink annihilate or reflect after a critical velocity. Moreover, the author proposed a reduced model describing the system using collective coordinates. Unfortunately, one of the equations had a typo that propagated in the literature for many years. In the triplet of papers [9–11] the authors computed the resonance windows for the ϕ^4 model, a modified sine-Gordon model, and the double sine-Gordon with high precision. Moreover, they argued that the resonance windows occur due to a resonant energy exchange mechanism between the kink’s translational and vibrational modes. Thus, They were able to find analytical expressions for the windows’ location and shape and conjecture that higher-order resonance windows exist at the border of the lower order ones. In [12] the authors showed that resonance windows form a fractal structure, both numerically and using the reduced system proposed by Sugiyama. Unfortunately, when the typo in the reduced equations was corrected, the qualitative similarity between the reduced and full systems disappeared [13]. After that, there has been a great number of works discussing kink-antikink interactions in various scenarios. Some of these include the investigation of quasinormal modes in kink-antikink collisions [14, 15], models with BPS preserving defects [16–21], interactions of kinks with fermions [22–26], collisions between kinks with long-rage tails [27–32], collision of kinks with boundaries [33–35], multikink scattering [36–39] and collision between kinks in two-component scalar field theories [40–42].

The double sine-Gordon model is a compelling non-integrable model which becomes integrable in some limits. Therefore, it is possible to study a gradual transition from integrability to non-integrability. A few important works about kink collisions in this model include [11, 39, 43, 44]. An important feature that appears in these works is that the kinks have an inner structure, that is, it consists of two subkinks, which may be exchanged at collision and form subkink bound states. This phenomenon was also observed in other systems with the kinks with inner structures [45]. Curiously, the double sine-Gordon model may effectively describe some physical systems such as gold dislocations [46], optical pulses and spin waves [47], pseudo 1-D ferromagnets [48] and Josephson structures [49]. Despite all that, it has not been sufficiently explored in the literature. It was only recently that the dependence of the critical velocity on the model parameter R was calculated [44].

Recently Alonso-Izquierdo et al. studied a fascinating problem for kink-antikink interactions [50]. They considered collisions between wobbling kinks, meaning that the kinks have their vibrational mode excited at the collision. The behavior of a single wobbling kink has already been studied [51–53]. In particular, it is well known that the wobbling amplitude decreases due to coupling to radiation. The collision between wobbling kinks is an important investigation because the second or higher collision in resonance windows may be seen as one such collision. Interestingly, the authors showed in [50] that there appear many separate one-bounce windows due to the wobbling. Here, we study collisions between wobbling double sine-Gordon kink and antikink. We show that the double sine-Gordon shares many similar features with the ϕ^4 model. We also show that the locations of the one-bounce windows are well approximated by the simplified analysis of the resonance windows structure of Campbell et al. Furthermore, this can also be visualized by plotting the maximum value of the energy densities similar to the analysis in [39, 54]. The structure of the paper is as follows. In section 2 we give a brief review of the double sine-Gordon models. In section 3 we show and compare the numerical results of our simulations of kink-antikink collisions with and without wobbling. Finally, in the last section, we give our concluding remarks.

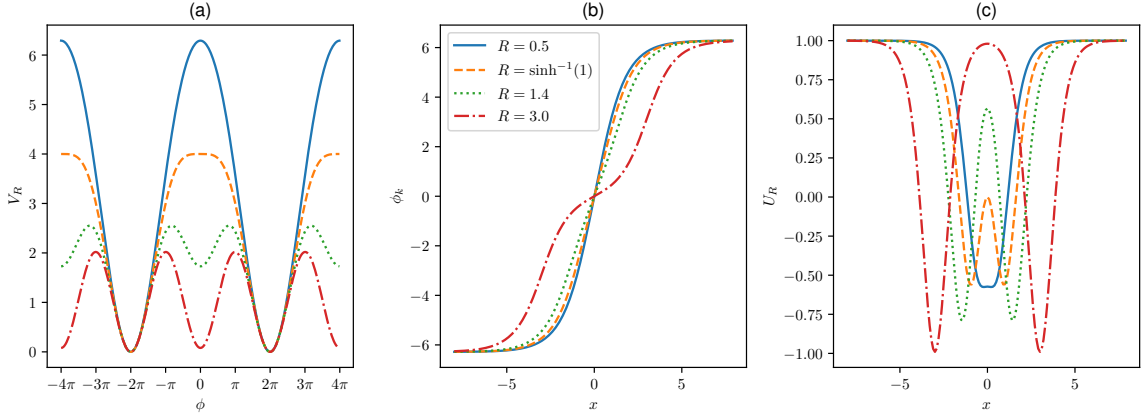


Figure 1: (a) Potential, (b) kink profile, and (c) linearized potential for the double sine-Gordon model with different values of the parameter R .

2 Model

Let us consider the double sine-Gordon model described by the following Lagrangian in (1+1) dimensions

$$\mathcal{L} = \frac{1}{2}(\partial_\mu \phi)^2 - V_R(\phi), \quad (1)$$

where ϕ is a scalar field and the potential term is given by [11]

$$V_R(\phi) = \tanh^2 R(1 - \cos \phi) + \frac{4}{\cosh^2 R} \left(1 + \cos \frac{\phi}{2}\right). \quad (2)$$

The potential is periodic and is shown in Fig. 1(a) for some values of R . It is clear from eq. (2) that for $R = 0$ and in the limit $R \rightarrow \infty$ the potential approaches the sine-Gordon one with periods 4π and 2π , respectively. For $\sinh^{-1}(1) \leq R \leq 0$, the potential has only one maximum per period, as in the sine-Gordon model. On the other hand, for $R > \sinh^{-1}(1)$, a local minimum appears, which approaches zero in the large R limit.

Solving the equation of motion of the system gives the following kink and antikink solutions (see Fig. 1(b))

$$\phi_{k(\bar{k})} = 4\pi n \pm 4 \tan^{-1} \left(\frac{\sinh x}{\cosh R} \right), \quad (3)$$

when the scalar field is static. If we write the sine-Gordon kink solution as $\phi_{SG} = 4 \tan^{-1} \exp(x)$, this becomes

$$\phi_{k(\bar{k})} = 4\pi n \pm [\phi_{SG}(x + R) - \phi_{SG}(R - x)]. \quad (4)$$

Therefore, one may interpret the double sine-Gordon kink as a superposition of two sine-Gordon kinks separated by a distance of $2R$.

We are interested in collisions between double sine-Gordon kinks that are vibrating. This is important to gain a deeper insight into the vibrational or shape modes' role in the resonance windows. Therefore, we look for these modes in the stability equation of the kink solution. Writing $\phi = \phi_k + \psi e^{i\omega t}$, where ψ is a small perturbation, leads to the Schrödinger-like equation

$$-\psi'' + U_R \psi = \omega^2 \psi, \quad (5)$$

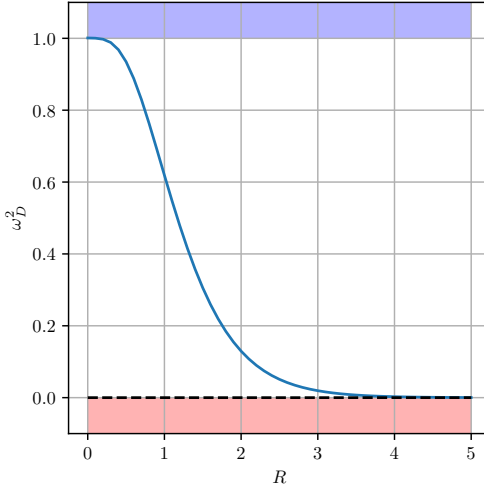


Figure 2: Spectrum of the linearized equation around a kink solution. The solid line is the vibrational mode, and the dashed line is the zero mode. The blue region represents the continuum region.

where the linearized stability potential is given by [44]

$$U_R = \frac{8 \tanh^2 R}{(1 + \operatorname{sech}^2 R \sinh^2 x)^2} + \frac{2(3 - 4 \cosh^2 R)}{\cosh^2 R (1 + \operatorname{sech}^2 R \sinh^2 x)} + 1. \quad (6)$$

The potential is shown in Fig. 1(c) for several values of R . For large R , it clearly splits into two sine-Gordon wells.

The spectrum of the linearized equation as a function of R is shown in Fig. 2. It contains a zero mode, as required by translational invariance, and a single vibrational mode. The normalized profile of the shape mode is denoted by ψ_D with eigenvalue ω_D^2 . It is simple to show that the energy stored in the shape mode with amplitude A is equal to $E_D = \frac{1}{2}\omega_D^2 A^2$. There is also a continuum of states starting at $\omega^2 = 1$. For $R = 0$ the vibrational mode disappears in the continuum, as the kink solution becomes the sine-Gordon one. For $R \gg 1$ the value of ω_D^2 approaches zero as the kink tends to two well-separated sine-Gordon kinks.

3 Collision simulations

To initialize the collision we take the following configuration

$$\phi = \phi_k(\xi_+) - \phi_k(\xi_-) - 2\pi + A \sin(\omega_D \tau_+) \psi_D(\xi_+) - A \sin(\omega_D \tau_-) \psi_D(\xi_-), \quad (7)$$

evaluated at $t = 0$. For the time evolution we defined the boosted coordinates $\xi_{\pm} = \gamma(x \pm x_0 \mp v_i t)$ and $\tau_{\pm} = \gamma(t \mp v_i x)$ ¹, where $\gamma = 1/\sqrt{1 - v_i^2}$. It consists of a kink and an antikink separated by a distance $2x_0$, fixed at the value $2x_0 = 30$. They approach each other with velocity v_i and $-v_i$, respectively, and at the same time, they wobble with the bound frequency ω_D^2 and amplitude A . For $A = 0$, this leads to the usual kink-antikink collision [11]. The technical details of the simulations are described in Appendix A.

¹It is a common mistake to only impose the boost on x coordinate and neglect it in the time coordinate.

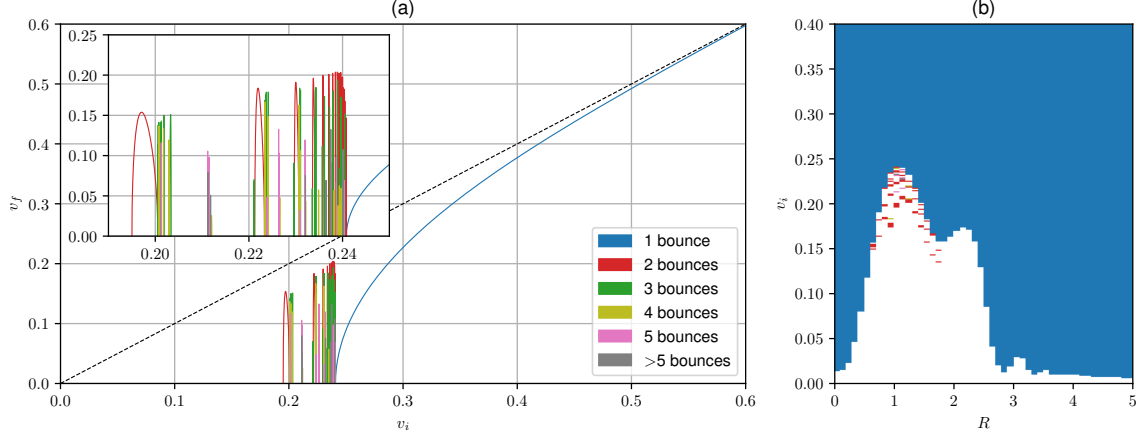


Figure 3: (a) Final velocity as a function of the initial velocity for kink-antikink collisions, considering $R = 1.0$. (b) Number of bounces before escape for kink-antikink collisions as a function of the initial velocity v_i and R . For both diagrams, we set $A = 0.0$.

From eq. (7), it is clear that the wobbling oscillation frequency is Lorentz contracted in the center of mass frame. If we measure the time evolution of the field at a point moving with the kink in the form $x = v_i t + \alpha$, the wobbling term becomes

$$A \sin \left(\frac{\omega_D}{\gamma} t - \gamma \omega_D v_i \alpha \right) \psi_D(\gamma(x_0 + \alpha)), \quad (8)$$

which oscillates with a Lorentz contracted frequency ω_D/γ . This transverse Doppler effect was also shown to appear in a more detailed description of wobbling kinks investigated in [52]. We will observe the same effect after the collision, where the frequency is contracted according to the system's final velocity.

The double sine-Gordon model with $A = 0$ exhibits resonance windows in a finite range of the parameter R . This occurs because, for both very small and very large R , the model becomes the sine-Gordon one, which does not have resonance windows. We show the final velocity as a function of the initial velocity for a specific value of $R = 1.0$ in Fig. 3(a). This value is in the region where the system exhibits resonance windows. The fractal structure is similar to the ϕ^4 model. However, there is a significant difference. Due to the periodicity of the potential, the kink and the antikink may either cross or reflect. An even number of bounces means that the kinks reflected, while an odd number means that the kinks crossed.

In Fig. 3(b), we show the number of bounces as a function of R and v_i , the initial velocity of the incoming kink-antikink. The colors represent the number of bounces as indicated in Fig. 3(a). The white region is where the kink and the antikink annihilate. In the blue region, separation occurs after a single bounce. Moreover, there is a region (approximately in the interval $0.6 \leq R \leq 1.7$) with dots in red and other colors with a fractal structure, which is the resonance domain. The interface between white and blue determines the critical velocity value, which agrees with the non-monotonic behavior reported in [44].

Now we would like to see how the result with $A \neq 0$ compares with the previous one. We start with a small value of $A = 0.1$. The final velocity dependence on the initial one is shown in Fig. 4(a) for $R = 1.0$. We observe that the blue crossing curve, which indicates separation after one-bounce, now oscillates as we vary v_i . This occurs because, for different velocities, the phase of the wobbling at the collision varies. Before the collision, the wobbling amplitude

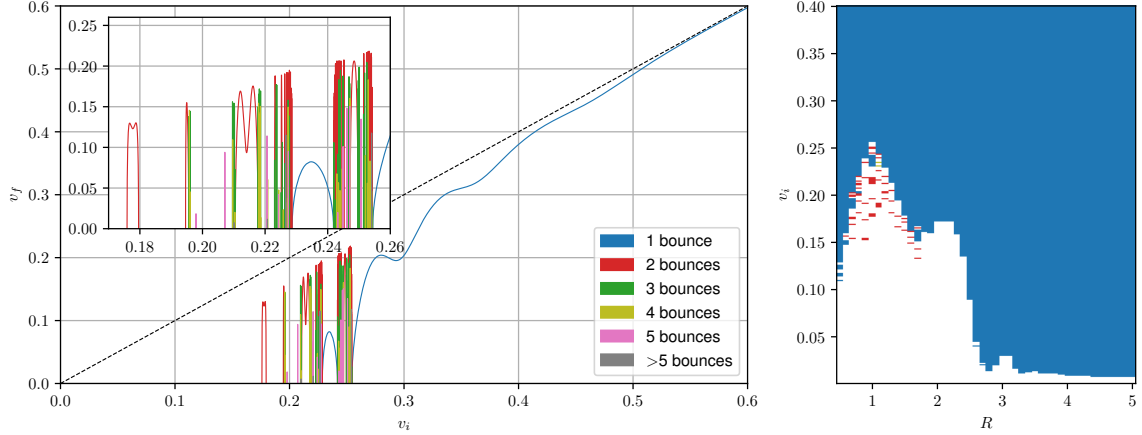


Figure 4: (a) Final velocity as a function of the initial velocity for kink-antikink collisions, considering $R = 1.0$. (b) Number of bounces before escape for kink-antikink collisions as a function of the initial velocity v_i and R . For both diagrams, we set $A = 0.1$.

evolves approximately as

$$S(t) = A \exp \left[i \left(\frac{\omega_D}{\gamma} t + \theta_0 \right) \right], \quad (9)$$

where θ_0 is an initial constant. Moreover, the collision occurs approximately at $t = x_0/v_i$. Therefore, the dependence of the phase θ at the collision on v_i can be estimated as

$$\theta = \sqrt{1 - v_i^2} \frac{\omega_D x_0}{v_i} + \theta_0. \quad (10)$$

Crossing after one bounce always occurs after a critical velocity. However, the oscillation in the amplitude, shown in eq. (9), causes the one-bounce crossing curve to split, creating one or more isolated one-bounce windows. Near these windows, there appears a nested structure of higher-bounce windows. The gap between the two one-bounce regions occurs because, in this region, the wobbling is out of phase at the collision time. Similarly, it is also possible to see oscillating behavior in some two-bounce windows. This novel phenomenon was also observed in the collision between wobbling kinks of the ϕ^4 model [50].

In Fig. 4(b), we summarize the behavior of the system for both dependences on R and v_i . It is possible to see that the one-bounce crossing region is split for a few values of R . The splitting gives rise to one-bounce resonance windows. In particular, the wobbling energy is enough to create one-bounce windows even for the values of R where there was no fractal behavior in the absence of wobbling, $A = 0$. One important detail is that in contrast with the case of $A = 0$, for small R it becomes difficult to find the shape mode profile numerically with enough precision as it approaches the continuum. That is the reason we have shown the figure starting with a small nonzero R .

For $A = 0.1$, the wobbling effect is small, while if we increase A , it becomes more pronounced. Figure 5(a) shows the system's behavior for a large wobbling amplitude $A = 0.8$. As one can see, there is an oscillating pattern in the curve of v_f as a function of v_i , as well as many isolated one-bounce resonance windows. This occurs in two ways. The first one is the process we described before. The one-bounce crossing curve is split in a region where the wobbling phase is such that the translational energy is lost at the collision. The second way is that a one-bounce window appears in a place where previously there was not any window. These windows show up because the energy transferred from the wobbling at the

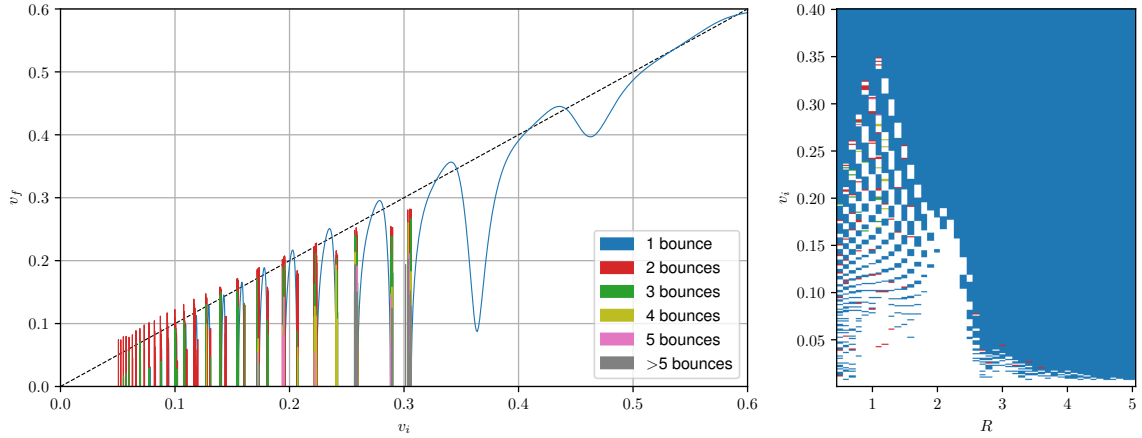


Figure 5: (a) Final velocity as a function of the initial velocity for kink-antikink collisions, considering $R = 1.0$. (b) Number of bounces before escape for kink-antikink collisions as a function of the initial velocity v_i and R . For both diagrams, we set $A = 0.8$.

collision is now high enough, letting the kinks separate. This phenomenon was also reported in [50] for the ϕ^4 model. Interestingly, near the boundary of a one-bounce window, there is a nested structure of higher-bounce windows. Furthermore, two essential features should be noticed. First, as we decrease v_i , the one-bounce resonance windows disappear, we see a pattern of two-bounce resonance windows that continues all the way down to zero initial velocity. Second, the final velocity may become higher than the initial one in some regions. Both features occur because the vibrational energy is considerable and, therefore, there is a large amount of energy available that may turn into translational energy at the collision.

The system's behavior for both dependences on R and v_i , although now with a larger wobbling amplitude $A = 0.8$, is summarized in Fig. 5(b). The figure shows an intricate structure of one-bounce resonance windows. This pattern shows that many one-bounce resonance windows appear for large values of A in the two ways previously described. In particular, we observe that the critical velocity after which one-bounce crossing always occurs is larger than the case with a smaller value of A . Due to the large amplitude of wobbling, when it is out of phase, there appear annihilation windows even for initial velocities as large as $v_i = 0.35$. These annihilation windows with large initial velocities are precisely where the final velocity curve for one-bounce crossing splits. Interestingly, we observe that one-bounce resonance windows appear in almost the whole region of R that we considered.

The one-bounce windows' behavior for the range $0 \leq A \leq 1$ and fixed value of $R = 1.0$ is summarized in Fig. 6(a). This is the best way to visualize the two processes of the creation of one-bounce windows. It is possible to see that gradually, as A is increased, the initial one-bounce curve splits, and new ones start to emerge. If A is large enough, whenever the vibration is in phase at collision, there are one-bounce resonance windows, while there are annihilation windows otherwise. A more detailed structure of n-bounce windows as a function of the system's relevant parameters is shown in Fig. 6(b). As one can see, the critical velocity and the number of isolated one-bounce windows increase as the amplitude of oscillation increases, consistent with Fig. 6(a) along with our arguments before. Moreover, the figure shows that the system also exhibits higher-bounce windows. However, the higher-bounce windows pattern is rather scarce because the higher-bounce resonance windows are narrow for the double sine-Gordon model. Nevertheless, it is also possible to see some higher-bounce resonance windows near the boundary of one-bounce resonance windows and in the

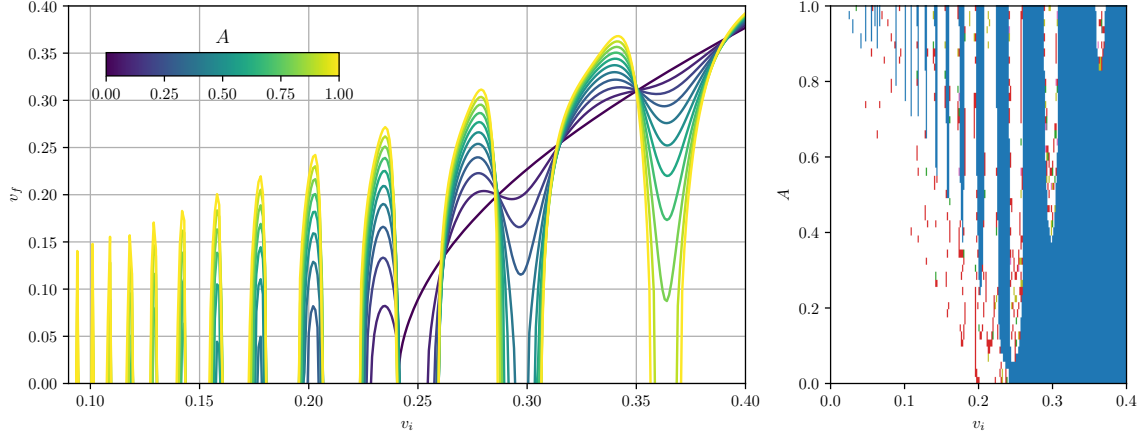


Figure 6: (a) Final velocity as a function of the initial velocity for kink-antikink collisions for different values of A . We fix $R = 1.0$. (b) Number of bounces before escape for kink-antikink collisions as a function of the initial velocity v_i and A .

region where A is large and v_i is small. In fact, it is easier to visualize this phenomenon in Fig. 5 for $A = 0.8$ where higher-order bounce windows accumulate in these two regions. Furthermore, the alternation between one-bounce and annihilation windows is clearly shown in Fig. 6(b) when A is large. This alternation depends on the wobbling phase right before the first collision, given by eq. (10).

We can find an approximate expression for the location of the one-bounce windows using the method proposed by Campbell et al. [9, 11]. Assuming that the amplitude is small and the system is invariant under time reversal, the authors found that the wobbling amplitude after the collision S' is approximately given by

$$S' = -\frac{\rho}{\rho^*} S + \rho, \quad (11)$$

where ρ is a complex constant that depends on the critical velocity. The center of the one-bounce windows should be located approximately at the point where the amplitude of wobbling is minimum. Plugging eq. (10) in eq. (11) we find

$$S' = -A \exp \left[i \left(\sqrt{1 - v_i^2} \frac{\omega_D x_0}{v_i} + \theta_0 + 2\theta_\rho \right) \right] + |\rho| \exp(i\theta_\rho), \quad (12)$$

where θ_ρ is the argument of ρ . The amplitude S' has a minimum absolute value for initial velocities v_n such that

$$\sqrt{1 - v_n^2} \frac{\omega_D x_0}{v_n} + \theta_0 + 2\theta_\rho = 2\pi n + \theta_\rho \quad (13)$$

for some integer n . More explicitly we have

$$v_n = \frac{\omega_D x_0}{\sqrt{(2\pi n - \delta)^2 + \omega_D^2 x_0^2}}, \quad (14)$$

where $\delta \equiv \theta_\rho + \theta_0$. Notice that the location of the centers is almost independent of the amplitude A , as can be observed in Fig. 6. Therefore, we choose $A = 1.0$ to measure the center of the one-bounce windows because there are more windows for this value. Figure 7

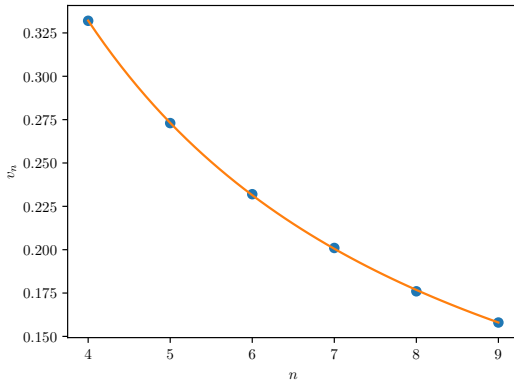


Figure 7: One-bounce windows center v_n as a function of the integer n for $R = 1.0$. The solid curve is a fit of the type given in eq. (15).

shows the centers of the one-bounce windows as a function of an integer n for $R = 1.0$. Fitting a curve of the type

$$v_n = \frac{a}{\sqrt{(2\pi n - b)^2 + a^2}}, \quad (15)$$

where a and b are fitting parameters, we find $a \simeq 9.22$, which should be compared to the theoretical value $\omega_D x_0 \simeq 11.80$. The agreement is not remarkable, which is expected given all the approximations in the equations. However, the above analysis gives a correct qualitative picture of the exact, within the numerical precision, numerical simulations.

Let us also study the maximum energy densities as a function of the system's parameters as reported in [39, 45]. The energy density is given by $e = k + u + p$ where the three terms in this expression are the kinetic $k = \frac{1}{2}(\partial_t \phi)^2$, gradient $u = \frac{1}{2}(\partial_x \phi)^2$ and potential $p = V(\phi)$ energy densities, respectively. During the collision, each of them will reach a maximum value, which we denote by a subscript *max*, at some position in spacetime. Figure 8 shows the maximum energy densities as a function of v_i and R in both scenarios with and without wobbling. In all the figures, we observe that, interestingly, the maximum energy densities vary smoothly inside the resonance windows, as shown in the highlighted one-bounce and two-bounce regions. This behavior is in clear contrast with erratic behavior in most points outside the resonance windows related to the bion formation, which is known to evolve chaotically [12]. The result in Fig. 8(b) matches the analogous figure in reference [39]. The double sine-Gordon is well known to form long-lived bound states, called oscillons, between the sine-Gordon subkinks. As far as we checked, the dependence of the maximum energy density on the initial velocity is also smooth in the regions where there is oscillon formation.

Finally, we would like to conclude with the measurement of the final wobbling frequency ω_f , the wobbling frequency of the system after the collision. We measure the final frequency by taking the field's value at a distance from the center, where the amplitude of wobbling has a maximum theoretical value. Then we subtract the kink contribution from the field and take the Fast Fourier of the evolution of this value. The frequency with the largest amplitude in the power spectrum is plotted in Fig. 9. In the figure, we divide the obtained frequency by $\sqrt{1 - v_f^2}$ to compensate the Lorentz contraction factor and change to the frame where the kink is at rest, as explained before. It is clear from the figure that, in this frame, the kink indeed wobbles at the shape mode's theoretical frequency ω_D . This result serves as a nice consistency check and is similar to what was obtained in [50] for the ϕ^4 model. Moreover,

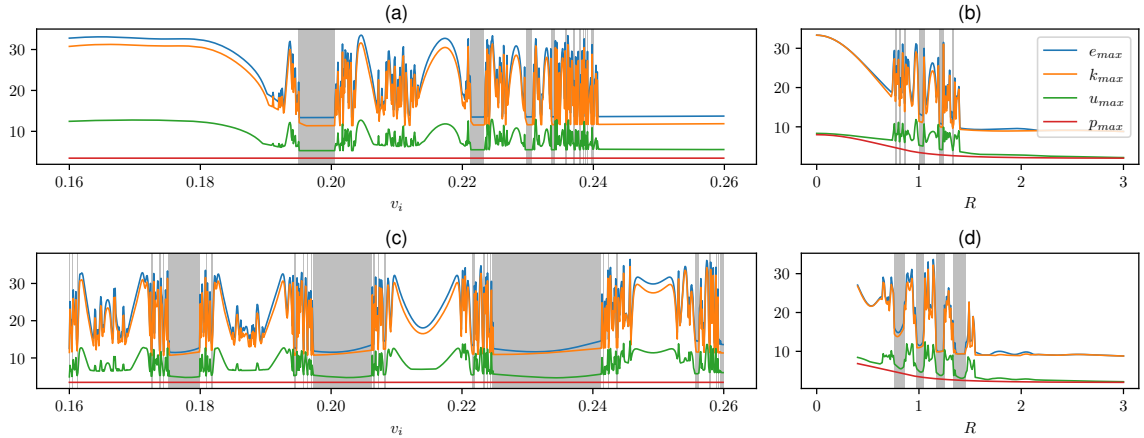


Figure 8: Maximum energy densities as a function of (a) v_i taking $R = 1.0$ (b) R taking $v_i = 0.2$, both for $A = 0.0$. (c) and (d) same quantities now with $A = 0.5$. The marked regions consist of one-bounce and two-bounce resonance windows.

higher-order effects in the amplitude can change the wobbling frequency from the lowest order value ω_D [52]. However, this effect is negligible compared with the Lorentz contraction one, consistent with the results in Fig. 9.

4 Conclusion

In this paper, we started with a subset of the double sine-Gordon model that depends on the parameter R . This model is well-known and coincides with the sine-Gordon model for $R = 0$ and in the limit $R \rightarrow \infty$. The model has at maximum one shape mode in the whole range of parameters, which is important for the appearance of resonance windows. Then, we investigated collisions between the kink and antikink in this model. The collisions exhibit the familiar fractal structure of resonance windows when the system is far from the integrable limits. Furthermore, we observed the previously reported non-monotonic critical velocity dependence on R .

Next, we added wobbling to the kink and antikink and studied collisions again. We found that the final velocity depends on the wobbling phase in an oscillatory way. If the wobbling is in phase in the first collision, we may observe a one-bounce crossing. This gives rise to separation after a critical velocity and also to isolated 1-bounce windows, which do not occur in the absence of wobbling. On the other hand, if the wobbling is out of phase, it causes annihilation or the formation of higher-bounce resonance windows. This phenomenon is even more pronounced for larger wobbling amplitudes, where we clearly see an alternating structure of these two behaviors. This result was found for a wide range of R and is similar to what was reported in [50] for the ϕ^4 model. However, in our case, every bounce corresponds to the kink-antikink crossing instead of reflecting. An interesting result is that the one-bounce windows' peak has a simple dependence on the wobbling phase. It can be found approximately considering a linear relation between the wobbling amplitude before and after the collision.

We measured the wobbling frequency of the kinks after the collision and found that indeed the kink wobbles at the theoretical value of the frequency ω_D once you change to the frame where the kink is at rest. This Lorentz contraction is manifest in our equation for a boosted

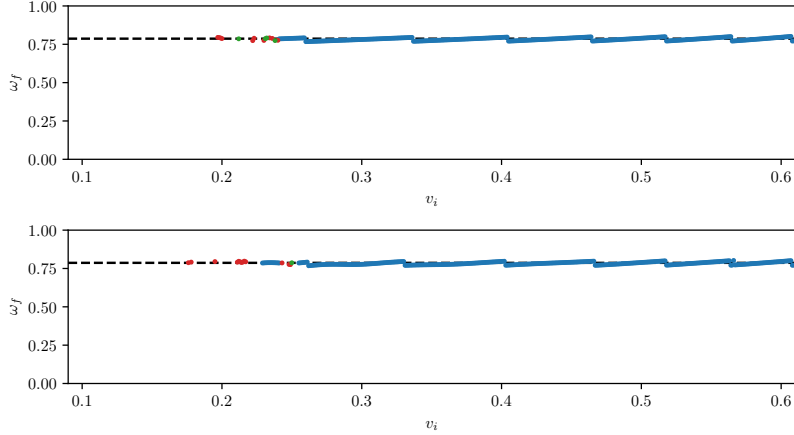


Figure 9: Final wobbling frequency as a function of the initial velocity for $A = 0.0$ (top) and $A = 0.1$ (bottom) with $R = 1.0$. The frequency was measured in the reference frame with the kink at rest, where the Lorentz contraction factor is compensated. The dashed line is the theoretical frequency of the shape mode $\omega_D \simeq 0.7867$. The color scheme represents the number of bounces as in previous figures.

wobbling kink.

The maximum energy density in the kinks collisions is an interesting way of studying the fractal structure of resonance windows [39, 45]. Curiously, we were able to show that it also works for our system. The energy density shows smooth behavior in the windows, independent of the parameters of the system, despite the chaotic structure of the collision. As far as we understand, the erratic behavior outside the windows is related to the bion formation. Moreover, in some of the smooth regions outside the resonance windows, we observed oscillon formation. However, to conclude that this is indeed the case whenever there is an oscillon formation needs a more thorough investigation.

This study helps to fill the gap in understanding the mechanism of resonance windows formation lacking in the energy exchange mechanism of Campbell et al. This simple mechanism is only an approximation because kink-antikink collisions are time-dependent phenomena with no well-defined wobbling state when the two mostly superpose. On the other hand, this work shows that wobbling has a notorious effect on the collision because its energy can easily turn into translational energy when the timing is right. Therefore, a more precise mechanism has to also account for this strong coupling between wobbling and translation.

A Numerical technique

To solve the equations of motion numerically, we discretize the space in the interval $-100.0 < x < 100.0$ using $N = 2048$ gridpoints and periodic boundary conditions. The space derivative is done using a Fourier spectral method [55] and the time evolution integrated using a 5th order Runge-Kutta method with error control [56] implemented with the `odeint` package in C++ [57]. We evolve the system until the time $t = 1400.0$. Hence, we cannot find resonance windows for very small velocities since there is not enough time for the kinks to separate. The radiation at the boundaries was absorbed by including a damping term in the region $x < -80$ and $x > 80.0$. The damping is proportional to a bump function with a maximum value of 5 and is exactly zero outside this region [31]. A larger box was used to compute the

final wobbling frequency to allow for a longer time series and obtain a more precise frequency measurement. The profile of the shape mode $\psi_D(x)$ was computed using the NDEigensystem method in Mathematica.

Acknowledgments

We acknowledge financial support from the Brazilian agencies CAPES and CNPq. AM also thanks financial support from Universidade Federal de Pernambuco Edital Qualis A. We thank Mauro Copelli for the access to his lab's computer cluster, which was essential for conducting the research reported in this paper.

References

- [1] Ramamurti Rajaraman. *Solitons and instantons*. North Holland, 1982.
- [2] Nicholas Manton and Paul Sutcliffe. *Topological solitons*. Cambridge University Press, 2004.
- [3] W_P Su, JR Schrieffer, and Ao J Heeger. Solitons in polyacetylene. *Physical review letters*, 42(25):1698, 1979.
- [4] Tanmay Vachaspati. *Kinks and domain walls: An introduction to classical and quantum solitons*. Cambridge University Press, 2006.
- [5] RD Yamaletdinov, VA Slipko, and YV Pershin. Kinks and antikinks of buckled graphene: A testing ground for the φ^4 field model. *Physical Review B*, 96(9):094306, 2017.
- [6] Mehran Kardar. *Statistical physics of fields*. Cambridge University Press, 2007.
- [7] Grigory E Volovik. *The universe in a helium droplet*, volume 117. Oxford University Press on Demand, 2003.
- [8] Tadao Sugiyama. Kink-antikink collisions in the two-dimensional φ^4 model. *Progress of Theoretical Physics*, 61(5):1550–1563, 1979.
- [9] David K Campbell, Jonathan F Schonfeld, and Charles A Wingate. Resonance structure in kink-antikink interactions in φ^4 theory. *Physica D: Nonlinear Phenomena*, 9(1-2):1–32, 1983.
- [10] Michel Peyrard and David K Campbell. Kink-antikink interactions in a modified sine-gordon model. *Physica D: Nonlinear Phenomena*, 9(1-2):33–51, 1983.
- [11] David K Campbell, Michel Peyrard, and Pasquale Sodano. Kink-antikink interactions in the double sine-gordon equation. *Physica D: Nonlinear Phenomena*, 19(2):165–205, 1986.
- [12] Peter Anninos, Samuel Oliveira, and Richard A Matzner. Fractal structure in the scalar $\lambda (\varphi^2 - 1)^2$ theory. *Physical Review D*, 44(4):1147, 1991.
- [13] I Takyi and H Weigel. Collective coordinates in one-dimensional soliton models revisited. *Physical Review D*, 94(8):085008, 2016.

- [14] Patrick Dorey and Tomasz Romańczukiewicz. Resonant kink–antikink scattering through quasinormal modes. *Physics Letters B*, 779:117–123, 2018.
- [15] João GF Campos and Azadeh Mohammadi. Quasinormal modes in kink excitations and kink–antikink interactions: a toy model. *The European Physical Journal C*, 80:1–15, 2020.
- [16] C Adam, T Romanczukiewicz, and A Wereszczynski. The ϕ^4 model with the bps preserving defect. *Journal of High Energy Physics*, 2019(3):131, 2019.
- [17] C Adam, K Oles, T Romanczukiewicz, and A Wereszczynski. Spectral walls in soliton collisions. *Physical review letters*, 122(24):241601, 2019.
- [18] Christoph Adam, Jose M Queiruga, and Andrzej Wereszczynski. Bps soliton-impurity models and supersymmetry. *Journal of High Energy Physics*, 2019(7):1–27, 2019.
- [19] Christoph Adam, K Oles, JM Queiruga, T Romanczukiewicz, and Andrzej Wereszczynski. Solvable self-dual impurity models. *Journal of High Energy Physics*, 2019(7):1–25, 2019.
- [20] NS Manton, Katarzyna Oleś, and Andrzej Wereszczyński. Iterated ϕ^4 kinks. *Journal of High Energy Physics*, 2019(10):1–16, 2019.
- [21] Christof Adam, K Oles, T Romanczukiewicz, and A Wereszczynski. Kink-antikink collisions in a weakly interacting ϕ^4 model. *Physical Review E*, 102(6):062214, 2020.
- [22] Gary Gibbons, Kei-ichi Maeda, and Yu-ichi Takamizu. Fermions on colliding branes. *Physics Letters B*, 647(1):1–7, 2007.
- [23] Paul M Saffin and Anders Tranberg. Particle transfer in braneworld collisions. *Journal of High Energy Physics*, 2007(08):072, 2007.
- [24] Yi-Zen Chu and Tanmay Vachaspati. Fermions on one or fewer kinks. *Physical Review D*, 77(2):025006, 2008.
- [25] Y Brihaye and T Delsate. Remarks on bell-shaped lumps: stability and fermionic modes. *Physical Review D*, 78(2):025014, 2008.
- [26] João GF Campos and Azadeh Mohammadi. Fermion transfer in the ϕ^4 model with a half-bps preserving impurity. *Physical Review D*, 102(4):045003, 2020.
- [27] Avinash Khare and Avadh Saxena. Family of potentials with power law kink tails. *Journal of Physics A: Mathematical and Theoretical*, 52(36):365401, 2019.
- [28] Ivan C Christov, Robert J Decker, A Demirkaya, Vakhid A Gani, PG Kevrekidis, and RV Radomskiy. Long-range interactions of kinks. *Physical Review D*, 99(1):016010, 2019.
- [29] Nicholas S Manton. Forces between kinks and antikinks with long-range tails. *Journal of Physics A: Mathematical and Theoretical*, 52(6):065401, 2019.
- [30] Ivan C Christov, Robert J Decker, A Demirkaya, Vakhid A Gani, PG Kevrekidis, Avinash Khare, and Avadh Saxena. Kink-kink and kink-antikink interactions with long-range tails. *Physical review letters*, 122(17):171601, 2019.

- [31] Ivan C Christov, Robert J Decker, A Demirkaya, Vakhid A Gani, PG Kevrekidis, and Avadh Saxena. Kink-antikink collisions and multi-bounce resonance windows in higher-order field theories. *arXiv preprint arXiv:2005.00154*, 2020.
- [32] João GF Campos and Azadeh Mohammadi. Interaction between kinks and antikinks with double long-range tails. *arXiv preprint arXiv:2006.01956*, 2020.
- [33] Robert Arthur, Patrick Dorey, and Robert Parini. Breaking integrability at the boundary: the sine-gordon model with robin boundary conditions. *Journal of physics A: mathematical and theoretical*, 49(16):165205, 2016.
- [34] Patrick Dorey, Aliaksei Halavanau, James Mercer, Tomasz Romanczukiewicz, and Yasha Shnir. Boundary scattering in the ϕ^4 model. *Journal of High Energy Physics*, 2017(5):107, 2017.
- [35] Fred C Lima, Fabiano C Simas, KZ Nobrega, and Adalto R Gomes. Boundary scattering in the ϕ^6 model. *Journal of High Energy Physics*, 2019(10):1–30, 2019.
- [36] Aliakbar Moradi Marjaneh, Vakhid A Gani, Danial Saadatmand, Sergey V Dmitriev, and Kurosh Javidan. Multi-kink collisions in the ϕ^6 model. *Journal of High Energy Physics*, 2017(7):28, 2017.
- [37] Aliakbar Moradi Marjaneh, Danial Saadatmand, Kun Zhou, Sergey V Dmitriev, and Mohammad Ebrahim Zomorrodian. High energy density in the collision of n kinks in the ϕ^4 model. *Communications in Nonlinear Science and Numerical Simulation*, 49:30–38, 2017.
- [38] Aliakbar Moradi Marjaneh, Alidad Askari, Danial Saadatmand, and Sergey V Dmitriev. Extreme values of elastic strain and energy in sine-gordon multi-kink collisions. *The European Physical Journal B*, 91(1):22, 2018.
- [39] Vakhid A Gani, Aliakbar Moradi Marjaneh, and Danial Saadatmand. Multi-kink scattering in the double sine-gordon model. *The European Physical Journal C*, 79(7):1–12, 2019.
- [40] A Halavanau, T Romanczukiewicz, and Ya Shnir. Resonance structures in coupled two-component ϕ^4 model. *Physical Review D*, 86(8):085027, 2012.
- [41] A Alonso-Izquierdo. Reflection, transmutation, annihilation, and resonance in two-component kink collisions. *Physical Review D*, 97(4):045016, 2018.
- [42] Alberto Alonso-Izquierdo. Non-topological kink scattering in a two-component scalar field theory model. *Communications in Nonlinear Science and Numerical Simulation*, 85:105251, 2020.
- [43] VA Gani and Alexander Evgenyevich Kudryavtsev. Kink-antikink interactions in the double sine-gordon equation and the problem of resonance frequencies. *Physical Review E*, 60(3):3305, 1999.
- [44] Vakhid A Gani, Aliakbar Moradi Marjaneh, Alidad Askari, Ekaterina Belendryasova, and Danial Saadatmand. Scattering of the double sine-gordon kinks. *The European Physical Journal C*, 78(4):345, 2018.

- [45] Yuan Zhong, Xiao-Long Du, Zhou-Chao Jiang, Yu-Xiao Liu, and Yong-Qiang Wang. Collision of two kinks with inner structure. *Journal of High Energy Physics*, 2020(2):1–21, 2020.
- [46] M El-Batanouny, S Burdick, KM Martini, and P Stancioff. Double-sine-gordon solitons: A model for misfit dislocations on the au (111) reconstructed surface. *Physical review letters*, 58(26):2762, 1987.
- [47] RK Bullough, PJ Caudrey, and HM Gibbs. The double sine-gordon equations: A physically applicable system of equations. In *Solitons*, pages 107–141. Springer, 1980.
- [48] A Rettori. Double-sine-gordon solitons in the ordered phase of the pseudo 1-d antiferromagnet k2fef5. *Solid state communications*, 57(8):653–655, 1986.
- [49] GL Alfimov, AS Malishevskii, and EV Medvedeva. Discrete set of kink velocities in josephson structures: The nonlocal double sine-gordon model. *Physica D: Nonlinear Phenomena*, 282:16–26, 2014.
- [50] A Alonso Izquierdo, J Queiroga-Nunes, and LM Nieto. Scattering between wobbling kinks. *Physical Review D*, 103(4):045003, 2021.
- [51] NS Manton and H Merabet. kinks-gradient flow and dynamics. *Nonlinearity*, 10(1):3, 1997.
- [52] IV Barashenkov and OF Oxtoby. Wobbling kinks in ϕ^4 theory. *Physical Review E*, 80(2):026608, 2009.
- [53] OF Oxtoby and IV Barashenkov. Resonantly driven wobbling kinks. *Physical Review E*, 80(2):026609, 2009.
- [54] Haobo Yan, Yuan Zhong, Yu-Xiao Liu, and Kei-ichi Maeda. Kink-antikink collision in a lorentz-violating ϕ^4 model. *Physics Letters B*, 807:135542, 2020.
- [55] Lloyd N Trefethen. *Spectral methods in MATLAB*. SIAM, 2000.
- [56] John R Dormand and Peter J Prince. A family of embedded runge-kutta formulae. *Journal of computational and applied mathematics*, 6(1):19–26, 1980.
- [57] Karsten Ahnert and Mario Mulansky. Odeint–solving ordinary differential equations in c++. In *AIP Conference Proceedings*, volume 1389, pages 1586–1589. American Institute of Physics, 2011.